ELECTRONIC SUPPLEMENTARY INFORMATION

METABOLIC SPATIAL VARIABILITY IN ELECTRODE-RESPIRING *GEOBACTER SULFURREDUCENS* BIOFILMS

Renslow RS[1†], Babauta JT[1], Dohnalkova A[2], Boyanov MI[3], Kemner KM[3], Majors PD[4], Fredrickson JK[4], and Beyenal H[1*]

[1] The Gene and Linda Voiland School of Chemical Engineering and Bioengineering, Washington State University, Pullman, Washington 99164, USA
[2] Environmental Molecular Sciences Laboratory, Pacific Northwest National Laboratory, Richland, Washington 99352, USA
[3] Biosciences Division, Argonne National Laboratory, Chicago, Illinois 60439, USA
[4] Biological Sciences Division, Pacific Northwest National Laboratory, Richland, Washington 99352, USA

* Corresponding author. Mailing address: The Gene and Linda Voiland School of Chemical Engineering and Bioengineering, Washington State University, 118 Dana Hall Spokane St., P.O. Box 642710, Pullman, WA 99164-2710. Phone: (509) 335-6607, Fax: (509) 335-4806. Email: beyenal@wsu.edu
† Current location: Environmental Molecular Sciences Laboratory, Pacific Northwest National Laboratory, Richland, Washington 99352, USA

ELECTRONIC SUPPLEMENTARY INFORMATION

Supplementary NMR Methods

2D/3D Fourier transform MRI. All 2D MRI data were collected using Bruker Paravision spin-echo method MSME. Face-plane 2DFT data employed field of view (FOV) dimensions of 10.24 mm by 5.12 mm. One hundred twenty-eight repetitions were collected with TE/TR (echo and repetition times) of 10.85/1000 milliseconds and 128 phase-encoding steps, for a total acquisition time of 4.5 hours. A total of 256 complex points were sampled at a rate of 200 Hz per pixel in the flow direction, with 128 phase-encoding steps in the lateral direction, for an in-plane resolution of 40 μm by 40 μm. The slice thickness was 3 mm. Axial-plane 2DFT data employed FOV dimensions of 5.12 mm by 5.12 mm. A total of 256 complex points were sampled at a rate of 200 Hz per pixel in the biofilm-normal direction, with 128 phase-encoding steps in the lateral direction, for a resolution of 40 μm by 40 μm. The slice thickness was 2 mm. Normal-plane 2DFT data employed FOV dimensions of 10.24 mm by 5.120 mm. A total of 256 complex points were sampled at a rate of 200 Hz per pixel in the flow direction, with 256 phase-encoding steps in the biofilm-normal direction, for an in-plane resolution of 40 μm by 20 μm. The slice thickness was 2 mm. All 2DFT scans employed Hermite 90-degree excitation pulses (10-kHz pulse bandwidth) and Hermite 180-degree radio frequency (RF) pulses (8 kHz RF pulse bandwidth). The 3DFT MRI employed Paravision's RARE spin-echo method with a TR/TE of 500 ms/8.43 ms. The FOV was 10.24 mm × 5.12 mm × 7.68 mm, with 256 complex points sampled in the flow direction at a 400-Hz frequency resolution and 128 and 192 independently sampled phase-encoding steps in the two remaining directions, for an isotropic spatial resolution of 40 μm. The total measurement time was ~27.6 h. Three-dimensional images were generated by Gaussian noise filtering and fast 3DFT processing.

Diffusion-mapping 2D Fourier transform MRI. Diffusion mapping employed Paravision method DtiStandard with the following parameter values: Repetition time: 500 ms; Echo time: 16.665 ms; Averages: 32; Pulse gradient width (∂): 3 ms; Diffusion time interval (Δ): 10 ms. The imaging sequence was repeated with seven different b-factors [0-1200 s/mm^2 in 200-s/mm^2 increments (aligned normal to the biofilm surface)] for a total measurement time of ~8 hr. Two-dimensional diffusion maps were generated by processing the individual images (Gaussian noise filtering followed by fast 2DFT processing) and then performing a semilogarithmic analysis of the b-factor-dependent intensity value of each image pixel above a preset noise threshold using a custom-written MATLAB script. Depth profiles were generated by averaging the pixels located in the middle 2 mm of the biofilm aligned with the flow direction.

Depth-resolved magnetic resonance spectroscopic imaging. Depth-resolved MRSI acetate profiles were collected using a gradient-echo 1D spectroscopic imaging method with "variable power RF pulses with optimized relaxation delays" (VAPOR) water suppression. Slice selection excitation was used to select a 3-mm-thick plane centered on the coverslip and normal to the flow direction. Depth profiling employed phase encoding in the direction normal to the coverslip with a FOV of 5.12 mm. For improved spatial localization, 409 phase encode (PE) steps were acquired with 65536 PE iterations, distributed over a Hanning function (a maximum of 76 PE averages were collected at the center of k space), and then Fourier transformed to 256 points, yielding a spatial (biofilm depth) resolution of 20 μm. A TR of 3000 ms was employed, for a total measurement time of ~54.6 hours. A total of 4096 complex data points were sampled with a

spectral window of 7 kHz. VAPOR employed Hermite pulses with 1500-Hz bandwidths. A second FT in the spectroscopic dimension yielded a two-dimensional dataset with a spatial dimension (biofilm and chamber depth) and a water-suppressed ^{1}H NMR spectral dimension. This corresponded to a depth-resolved metabolite map of the sample chamber and biofilm. Depth-resolved MRSI water profiles were also collected using a gradient-echo 1D spectroscopic imaging method (without VAPOR water suppression) in order to correct the acetate depth profiles based on the spatially resolved pore-space volume. The slice selection excitation, phase-encoding direction, FOV, data point sampling, and spectral window were identical to those used for the raw acetate profiles. A total of 305 PE steps were acquired with 512 PE iterations, distributed over a Hanning function (a maximum of 2 PE averages were collected at the center of k space), and then Fourier transformed to 256 points, yielding a spatial (biofilm depth) resolution of 20 μm. A TR of 15,000 ms was employed, for a total measurement time of ~2 hours. A single water-suppressed spectrum is shown in ESI Figure S1.

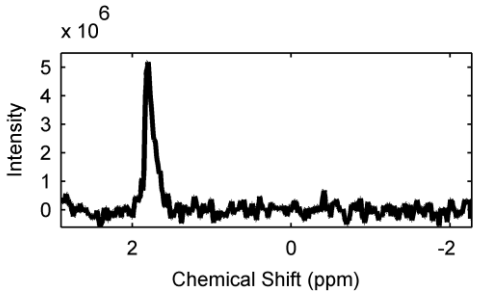

ESI Figure S1 | Example water-suppressed spectrum at a single depth. The gradient-echo 1D spectroscopic imaging method was used with VAPOR water suppression to generate acetate concentration depth profiles. This figure shows the proton spectrum at 760 μm above the base of the biofilm, representing the MRSI signal for acetate within a voxel 20 μm thick, 4 mm wide (width of NMR), and 2 mm deep . Integrating this spectrum over the acetate peak (chemical shift of ~1.9) and correcting the intensity based on the pore-space volume (obtained using non-water-suppressed MRSI) provided the local concentration datum for a single point (at 760 μm) in the Figure 2c acetate depth profile.

Supplementary X-ray Absorption Spectroscopy Results

ESI Figure S2a shows a map of the U L_{α}-line fluorescence intensity of a biofilm thin cross section. The biofilm-solution interface is at the top of the image, where several areas of high U concentration are observed. These areas correspond to the areas of high electron density seen in the TEM images in Figure 4d, as verified by TEM on thinner sample sections adjacent to the one examined using XRF analysis (data not shown). U L_{III}-edge XANES spectra were collected at the high U concentration areas marked by rectangles as areas 1, 2, and 3. The spectra are compared to each other and to a U^{IV} and a U^{VI} standard in ESI Figure S2b. The intermediate position of the sample spectra between the standards spectra indicates the presence of both U^{IV} and U^{VI}. The average U^{IV} content of the three areas was quantified as 45±10% of the total U in the beam using linear combination fitting of the spectra with the U^{IV} and U^{VI} standards. The presence of U^{VI} in the same areas as U^{IV} may indicate the formation of a mixed-valence U mineral during U^{VI} reduction, or it may indicate partial oxidation of the reduced U^{IV} during sectioning of the fixed biofilm, which was performed under ambient conditions. The presence of U^{IV} as determined by micro-XANES indicates the occurrence of electron transfer to U^{VI} in these areas of the biofilm.

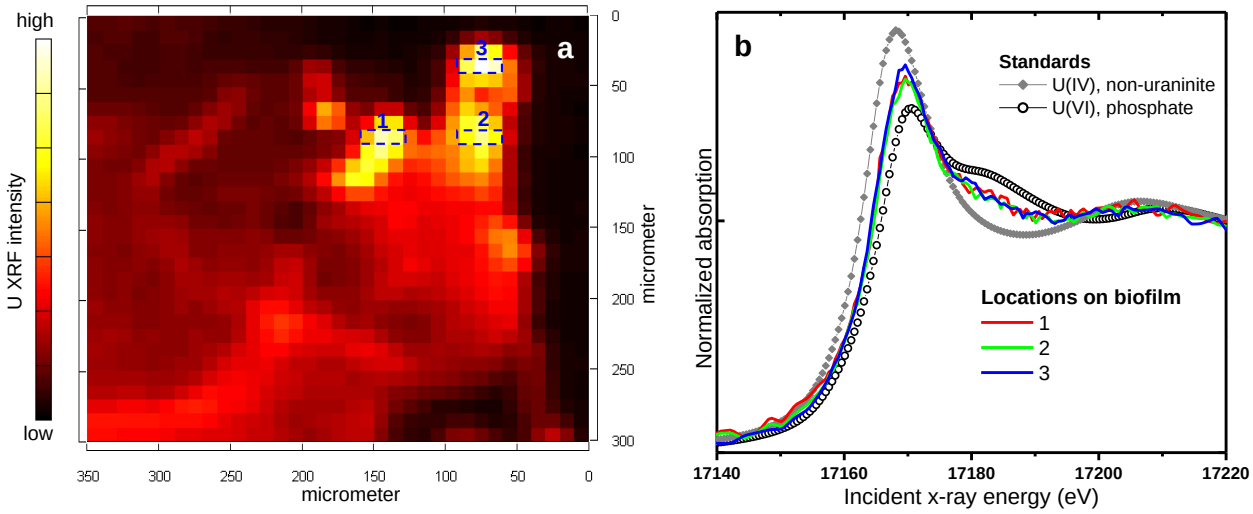

ESI Figure S2 | (a) U L_{α}-line X-ray fluorescence intensity map of the biofilm sample. The sample was probed with a 10x30-micron beam of 17,200-eV incident energy. The biofilm-solution interface is located at the top. Areas of high U concentration are shown in yellow-white colors. The beam size and three locations where XANES spectra were taken are noted. **(b) U L_{III}-edge XANES spectra from the locations in ESI Figure S2a.** XANES spectra from locations 1, 2, and 3, shown in ESI Figure S2a, compared to a U^{VI}-phosphate standard and the non-uraninite U^{IV}-phosphate phase observed in Boyanov *et al*. (2011)[1].

Supplementary Computational Modeling

A simple two-dimensional computation model was developed to provide a basis for hypothesis testing and to help interpret the experimentally determined NMR depth profiles. Two separate cases were simulated, one assuming that only the top of a 270-μm-thick *Geobacter sulfurreducens* biofilm was metabolically active ("top-active") and one assuming that only the base was metabolically active ("bottom-active"). The goal was to determine how the acetate concentration and flux profiles would look when certain regions were assumed to be active and to compare the model results with the actual NMR results that we obtained. The first case, in which only the top is active, represents a biofilm without any electron acceptor limitations, meaning that cells can transfer electrons to the gold electrode without any resistance. The second case, in which only the base is active, represents a biofilm that has electron transfer limitations for cells that are far from the electrode. Comsol Multiphysics (version number 4.2.1.166, COMSOL Inc., Burlington, MA, USA), a finite element method simulation package, was used to build and test the model. An 8-core, 64-bit Microsoft Windows 7 computer with 16 GB of RAM was used to run the simulation.

The model geometry was constructed to represent the NMR microimaging biofilm reactor, but was restricted to the area around the biofilm and the NMR measurement voxel. The height of the reactor was set to 2 mm, and the length was set to 20% of the actual length (8 mm), centered on the biofilm. Modeling only the middle 8 mm of the reactor produced an identical fluid flow profile and acetate concentration inside the NMR measurement voxel while significantly reducing computational time. The inlet boundary condition for fluid flow was defined to ensure that the fluid flow profile was laminar and matched the profile produced when a full-length reactor was simulated. Laminar flow was assumed because of the low Reynolds number of 0.1 for a flow of 1 mL/hr[2]. The biofilm was assumed to be a 270-μm-thick rectangular slab positioned on the 5-mm-diameter gold disc. Meshing of the two-dimensional domains (the EC-NMR biofilm reactor and the biofilm) was performed using free triangular mesh elements, each with a maximum element size of 20 μm. Mesh elements along the center edge used to create depth profiles were constrained to a maximum element size of 1 μm in order to generate smooth depth profile plots and to ensure a high element density where the profiles would be produced.

The modeling parameters, including fluid flow speed, inlet acetate concentration, and temperature, were identical to those of the experimental setup after the biofilm had reached a thickness of 270 μm. Acetate was fully oxidized inside the biofilm, assuming Monod behavior. The biofilm activity was set sufficiently high to allow for complete utilization of the acetate within the depth of the active region in order to represent the two extremes of a top-active and a bottom-active biofilm. A 30-μm-thick active region was positioned at the top or base of the biofilm, for the top-active or bottom-active simulation, respectively. A diffusion coefficient depth profile inside the biofilm was approximated by interpolating the data shown in Figure 2a (diffusion coefficient depth profile obtained via NMR for a 270-μm-thick biofilm) using piecewise cubic interpolation.

ESI Figure S3 shows the simulated acetate concentration and acetate molar flux depth profiles of a top-active and a bottom-active biofilm. For the top-active biofilm, the acetate concentration drops to zero within the biofilm; however, for the bottom-active biofilm the acetate concentration remains present within the biofilm and only reaches zero near the base of the biofilm. The flux profile of the top-active biofilm drops quickly within the biofilm and remains at zero inside the biofilm. For the bottom-active biofilm the flux remains flat and nonzero within

the biofilm and only drops near the base. This demonstrates that for a bottom-active biofilm, there is no reaction occurring within the biofilm except for near the base. Comparing these results to the actual NMR data leads us to hypothesize that our 270-μm-thick biofilm was not actively metabolizing near the base but was metabolically active in the middle and near the top of the biofilm. Based on the flux profile in Figure 2d, the bottom 37% of our biofilm was restricted from acetate, which was consumed within the top 63% of the biofilm. Several features from the model corroborate that the NMR experimental data do indeed reveal a biofilm with cells near the top that are able to oxidize acetate and utilize a distant electron-accepting electrode:

1. Acetate is consumed to undetectable limits inside the biofilm (not near the base)
2. Acetate flux is not constant (flat) near the top of the biofilm
3. Acetate flux quickly goes to zero inside the biofilm, corresponding to a lack of acetate and therefore metabolism
4. Acetate flux is zero inside the biofilm and remains so to the base

As the biofilm ages, the thickness increases as well as the distance from the base, where the acetate is consumed (Figure 4). This only further confirms that the top of the biofilm is metabolically active and provides additional evidence of long-range electron transfer. The mathematical model allowed us to test two extreme scenarios and show that our data do indeed support the hypothesis of biofilm activity beyond just a few tens of microns from the base of the biofilm.

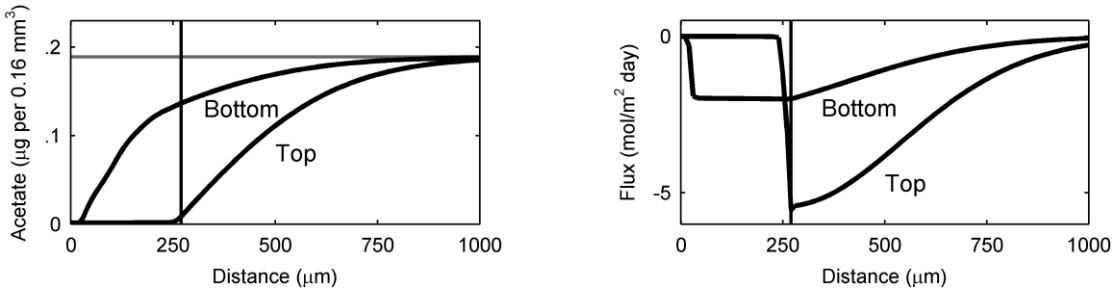

ESI Figure S3 | Computational modeling. Results shown for two cases: a top-active biofilm and a bottom-active biofilm, as designated by the text in each panel. Left) Depth profile of acetate concentration versus the distance from the base of the biofilm. The grey horizontal line indicates the acetate concentration provided in the growth medium. The black vertical line represents the biofilm/bulk liquid interface at 270 μm. Right) Depth profile of acetate molar flux.

1. M. I. Boyanov, K. E. Fletcher, M. J. Kwon, X. Rui, E. J. O'Loughlin, F. E. Löffler and K. M. Kemner, *Environmental Science & Technology*, 2011, **45**, 8336-8344.

2. R. S. Renslow, P. D. Majors, J. S. McLean, J. K. Fredrickson, B. Ahmed and H. Beyenal, *Biotechnol. Bioeng.*, 2010, **106**, 928-937.